

Lateral stiffness: A new nanomechanical measurement for the determination of shear strengths with friction force microscopy

R. W. Carpick,^{a)} D. F. Ogletree, and M. Salmeron^{b)}

Materials Sciences Division, Lawrence Berkeley National Laboratory, Berkeley, California 94720

(Received 21 November 1996; accepted for publication 20 January 1997)

We present a technique to measure the lateral stiffness of the nanometer-sized contact formed between a friction force microscope tip and a sample surface. Since the lateral stiffness of an elastic contact is proportional to the contact radius, this measurement can be used to study the relationship between friction, load, and contact area. As an example, we measure the lateral stiffness of the contact between a silicon nitride tip and muscovite mica in a humid atmosphere (55% relative humidity) as a function of load. Comparison with friction measurements confirms that friction is proportional to contact area and allows determination of the shear strength. © 1997 American Institute of Physics. [S0003-6951(97)01412-5]

The friction force microscope (FFM)¹ has emerged as an important tool to study nanotribology—the atomic scale origins of friction, adhesion, lubrication, and wear.² Recent observations indicate that at low loads, the FFM tip can form a single asperity contact with a surface^{3–6} and wearless interfacial sliding occurs. Friction appears to scale with load in proportion to the area of contact as predicted for a continuous, elastic, single asperity contact. In other words,

$$F_f = \tau A = \tau \pi a^2, \quad (1)$$

where F_f is the frictional force, A the contact area, a the contact radius, and τ the shear strength (shear force/area), in contrast to the macroscopic observation of friction being proportional to load (due to multiple asperity contact⁷ and/or wear or plastic deformation⁸). However, contact area is not directly measured with FFM, so a contact mechanical model must be chosen to properly investigate the relationship between friction and contact area. The particular model utilized, such as the Hertz⁹ or Johnson–Kendall–Roberts¹⁰ model, depends upon the strength and range of the tip-sample interaction forces¹¹ (among other things), which is uncertain in each case. The contact area-load relation for a single asperity also depends upon the tip shape, as demonstrated experimentally by Carpick *et al.*⁶ Furthermore, if the shear strength is not independent of load (pressure), then the load dependence of shear strength and contact area become convoluted.⁴ As well, the models used neglect the effect of lateral forces upon the contact area, yet this may indeed be a significant effect^{12,13} to explore. For these reasons, an independent measurement related to the contact area is desirable.

Contact stiffness is defined as the amount of force per unit displacement required to compress an elastic contact in a particular direction, has the units of N/m, and is essentially the “spring constant” of the contact. For example, the normal stiffness is given by $\kappa = dL/dz$, where L is the applied load (normal force), and z is the elastic penetration depth. In the Hertz case⁹ (an elastic sphere-plane contact),

$$\kappa_{\text{contact}} = 2 a E^*, \quad (2)$$

where $E^* = [(1 - \nu_1^2)/E_1 + (1 - \nu_2^2)/E_2]^{-1}$; E_1 and E_2 are the Young’s moduli of the sphere and plane, respectively, and ν_1 and ν_2 the respective Poisson’s ratios. From Eq. (2), the normal stiffness is directly proportional to the contact radius, which for the Hertz case is given by $a = (3RL/4E^*)^{1/3}$, where R is the sphere radius (the sphere is approximated as a paraboloid). Typically the contact strain is concentrated within a volume of the order a^3 .

With FFM, the plane corresponds to the sample, and the sphere corresponds to the tip. In addition, the sphere is attached to a spring, i.e., the cantilever, which has its own stiffness (the normal spring constant κ_{lever}). The cantilever and the contact are thus two springs in series [Fig. 1(a)]. For nanometer-sized contacts between common materials like metals and ceramics, stiffness values are roughly 50–500 N/m. However, the normal stiffness of typical commercial FFM cantilevers, κ_{lever} , is on the order of 0.01–1 N/m. Thus nearly all the elastic compression is taken up by the lever and not the contact, so the measurement is relatively insensitive to κ_{contact} . Notably, Pethica and co-workers¹⁴ have designed a substantially modified scanning force microscope using custom-made cantilevers where a magnetic force is directly applied to the tip. With this setup, the normal stiffness can be sensitively measured.

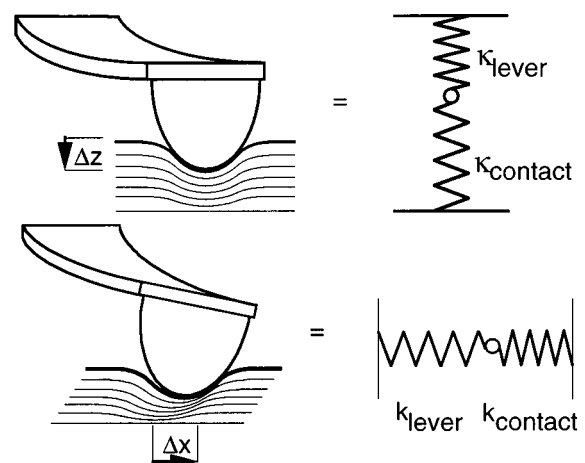


FIG. 1. Model showing normal and lateral stiffnesses in FFM.

^{a)}Also at Department of Physics, University of California at Berkeley, Berkeley, California.

^{b)}Author to whom correspondence should be sent. Phone: (510) 486-6704; fax (510) 486-4995. Electronic mail: salmeron@stm.lbl.gov

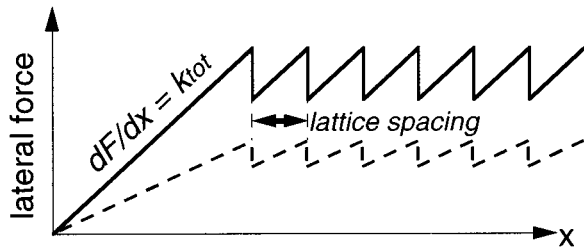


FIG. 2. Lateral force signal vs lateral displacement (x). Solid line: a relatively stiff contact. Dashed line: a softer contact—there is less cantilever bending per unit displacement since the contact is being substantially compressed.

However, the typical *lateral* stiffness of commercial FFM cantilevers, k_{lever} , is around 50–200 N/m,¹⁵ i.e., of the same order as the lateral contact stiffness, k_{contact} , so typical cantilevers can accurately measure variations in the *lateral* stiffness of nanometer-sized contacts, i.e.,

$$\frac{dF_{\text{lateral}}}{dx} = k_{\text{tot}} = \left[\frac{1}{k_{\text{lever}}} + \frac{1}{k_{\text{contact}}} \right]^{-1}, \quad (3)$$

where F_{lateral} is the lateral force (cantilever torsion), and x is the lateral displacement [Fig. 1(b)]. For a sphere-plane contact, k_{contact} is given by¹⁹

$$k_{\text{contact}} = 8 G^* a, \quad (4)$$

where $G^* = [(2 - \nu_1)/G_1 + (2 - \nu_2)/G_2]^{-1}$. Here G_1 and G_2 are the tip and sample shear moduli, respectively. Again, k_{contact} is directly proportional to the contact radius. A further advantage is that Eq. (4) holds, regardless of the tip-sample interaction forces,¹⁶ unlike the analogous equation for normal stiffness, Eq. (2), which must be modified for non-Hertzian contacts.

A simple explanation of Eq. (4) is obtained by considering an applied lateral force dF_{lateral} at fixed load, i.e., applying a lateral stress $d\sigma$ over the contact area A , producing a proportional strain $d\epsilon$, where $d\epsilon \propto dx/a$ (since a is the length scale of the stress distribution). Stress and strain are related by Hooke's Law, $d\sigma = G \times d\epsilon$, where G is the shear modulus, appropriate for the direction of the applied stress considered here. Hence $dF_{\text{lateral}}/A \propto G \times dx/a$, giving $dF_{\text{lateral}}/dx \propto G \times a$ as in Eq. (4). Note the simplifying assumption that the contact radius is not affected by the lateral displacement dx . This is reasonable and expected for small lateral displacements.¹⁶ In the case of normal stiffness, the normal displacement dz *does* change the contact radius, which essentially explains why normal stiffness is not generally proportional to contact radius (except in the Hertz case). The relation between lateral stiffness and energy dissipation from friction has been discussed by Colchero *et al.*¹⁷

As long as there is finite static friction between the tip and sample, the lateral stiffness can be measured. Consider the lateral force response of a cantilever as it scanned across a sample (Fig. 2). Typically, atomic scale stick-slip behavior is preceded by an initial sticking portion, the slope of which corresponds to $dF_{\text{lateral}}/dx = k_{\text{tot}}$, the total lateral stiffness. To measure this slope accurately, the relative lateral position between the cantilever base and the sample is sinusoidally modulated with an amplitude small enough, typically a few

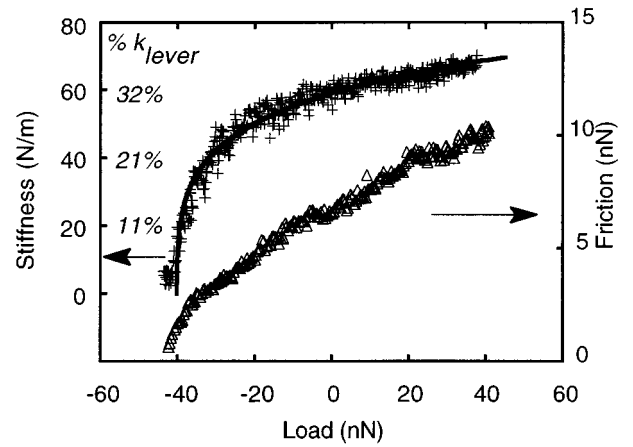


FIG. 3. Crosses: lateral stiffness (k_{tot}) vs load data. Solid line: a fit of the shifted Hertz model [Eq. (5)]. As load increases, k_{tot} asymptotically approaches k_{lever} , (~ 190 N/m, from the fit), although, even at the maximum load, $k_{\text{tot}} \sim 35\% k_{\text{lever}}$. Triangles: F_f vs load, acquired shortly after the stiffness measurement.

angstroms, to avoid slip even at low loads. A lock-in amplifier is used to measure the amplitude of the lateral force response over a range of loads. If slip occurs, a significant out-of-phase lock-in response results. A two channel lock-in can monitor the out-of-phase component, to discard measurement points where slip occurred. This will be discussed in more detail elsewhere¹⁸ and was not necessary for this example. The in-phase amplitude (dF_{lateral}) divided by the amplitude of relative displacement (dx , determined by accurately knowing the piezo response calibration) corresponds to the *total* lateral stiffness of the system, k_{tot} [Eq. (3)]. Using a similar setup, Colchero *et al.*¹⁹ measured friction by using a large lateral displacement amplitude so that sliding took place. For our measurements, a silicon nitride Digital Instruments²⁰ cantilever with a nominal normal force constant ~ 0.58 N/m was used.

Lateral stiffness (k_{tot}) was measured versus load for the tip contacting freshly cleaved muscovite mica in humid atmosphere [$\sim 55\%$ relative humidity (RH)] (Fig. 3 - crosses). The k_{tot} shows a distinct load dependence with a good signal to noise ratio. The fit (Fig. 3 - solid line) indicates how k_{tot} should vary with load (also fitting a value for k_{lever}), using the Hertz theory with the load axis shifted by the critical load L_c (pull-off force),

$$a = \left[\frac{3R}{4E^*} (L + L_c) \right]^{1/3}. \quad (5)$$

This dependence is predicted by Fogden and White²¹ for an elastic contact in the presence of capillary condensation for appropriate values of the elastic constants, tip radius, and relative humidity. Using their model, we have determined that Eq. (5) should apply in our case. A more detailed discussion of this approach has been presented elsewhere.⁴ Note from Fig. 3 that k_{tot} only reaches 35% of k_{lever} at the highest load; the contact deformation is equal to or greater than the lateral lever deformation at loads and conditions typically encountered in FFM experiments.¹⁷

We emphasize that no model needs to be chosen to determine the shear strength τ of the contact. To do this, fric-

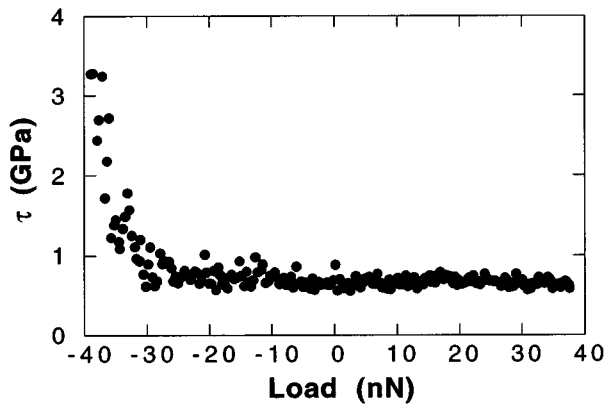


FIG. 4. The total stiffness τ vs load from the stiffness and friction data in Fig. 3.

tion was measured as a function of load immediately after the stiffness measurement (Fig. 3 - triangles) using a standard technique described elsewhere.^{3,6,22} To see how τ varies with load, Eqs. (1), (3), and (4) are combined to give

$$\tau = \frac{64 G^*{}^2 F_f}{\pi k_{\text{contact}}^2} \quad (6)$$

We calculate and plot $64 \cdot G^*{}^2 \cdot F_f / \pi \cdot k_{\text{contact}}^2$ at each load value from the separately acquired measurements of friction and stiffness (Fig. 4). The shear strength τ appears to be independent of load with a value of ~ 680 MPa, except near pull-off (~ -40 nN). We believe this low-load anomaly is due to water or hydrocarbon contaminants between the tip and sample which lead to low stiffness values at low loads,²³ and/or slippage occurring at low loads. We emphasize that this value for τ is an estimate as we rely upon bulk values of the elastic constants. These values are somewhat uncertain for the tip material, silicon nitride, because it is produced by chemical vapor deposition resulting in an amorphous structure with uncertain stoichiometry and residual stress. Our most informed estimate is $G_1 = 61$ GPa, $\nu_1 = 0.27$.^{24,25} The bulk values for mica are $G_2 = 13.5$ GPa, $\nu_1 = 0.10$.²⁶ Mica, having a significantly smaller shear modulus, influences G^* more strongly, giving $G^* = 5.9$ GPa. It is not known if the bulk values for elastic constants are valid at the nanometer scale (which could in fact be tested with this method), but recent nanomechanical measurements of gold indicate approximate agreement with bulk values.^{27,28} Unlike model-dependent methods, the tip radius is not needed to calculate τ . Note that if the tip is not parabolic, the coefficient of G^*a in Eq. (4) would be different. We confirmed this tip to be parabolic using the sharp edges of a faceted SrTiO₃(305) sample as described previously.^{6,29} A certain value for k_{lever} was assumed above. Methods to determine k_{lever} if calibration uncertainties exist will be discussed elsewhere, along with detailed comments on error analysis and further measurements at other humidities and in ultrahigh vacuum (UHV).¹⁸

In conclusion, we have described a fast and straightforward technique to determine the shear strength of a FFM tip-sample contact independent of contact mechanics models, by measuring the lateral contact stiffness. In general, friction and lateral stiffness measurements are complementary techniques which should be employed in tandem when studying nanotribology with FFM.

The authors gratefully acknowledge Professor K. L. Johnson for useful discussions and encouragement. R. W. C. acknowledges support from the Natural Sciences and Engineering Research Council of Canada. This work was supported by the Director, Office of Energy Research, Basic Energy Sciences, Materials Division of the U.S. Department of Energy under Contract No. DE-AC03-76SF00098.

- ¹C. M. Mate, G. M. McClelland, R. Erlandsson, and S. Chiang, Phys. Rev. Lett. **59**, 1942 (1987).
- ²*Fundamentals of Friction: Macroscopic and Microscopic Processes*, edited by I. L. Singer and H. M. Pollock (Kluwer, Dordrecht, 1992), Vol. 220.
- ³J. Hu, X.-D. Xiao, D. F. Ogletree, and M. Salmeron, Surf. Sci. **327**, 358 (1995).
- ⁴U. D. Schwarz, W. Allers, G. Gensterblum, and R. Wiesendanger, Phys. Rev. B **52**, 14976 (1995).
- ⁵E. Meyer, R. Luthi, L. Howald, M. Bamberlin, M. Guggisberg, and H.-J. Guntherodt, J. Vac. Sci. Technol. B **14**, 1285 (1996).
- ⁶R. W. Carpick, N. Agrait, D. F. Ogletree, and M. Salmeron, J. Vac. Sci. Technol. B **14**, 1289 (1996).
- ⁷J. A. Greenwood, in *Fundamentals of Friction*, edited by I. L. Singer and H. M. Pollock (Kluwer, Dordrecht, 1992), p. 111.
- ⁸F. P. Bowden and D. Tabor, *Friction and Lubrication of Solids: Part I* (Oxford University Press, 1950).
- ⁹K. L. Johnson, *Contact Mechanics* (University Press, Cambridge, 1987).
- ¹⁰K. L. Johnson, K. Kendall, and A. D. Roberts, Proc. R. Soc. London, Ser. A **324**, 301 (1971).
- ¹¹K. L. Johnson, Langmuir **12**, 4510 (1996).
- ¹²A. R. Savkoor, in Ref. 7, p. 111.
- ¹³K. L. Johnson, Proc. R. Soc. London Ser. A **543**, 163 (1997).
- ¹⁴S. P. Jarvis, A. Oral, T. P. Weihs, and J. B. Pethica, Rev. Sci. Instrum. **64**, 3515 (1993).
- ¹⁵D. F. Ogletree, R. W. Carpick, and M. Salmeron, Rev. Sci. Instrum. **67**, 3298 (1996).
- ¹⁶K. L. Johnson (personal communication).
- ¹⁷J. Colchero, A. M. Baro, and O. Marti, Trib. Lett. **2**, 327 (1996).
- ¹⁸R. W. Carpick, D. F. Ogletree, and M. Salmeron (unpublished).
- ¹⁹J. Colchero, M. Luna, and A. M. Baro, Appl. Phys. Lett. **68**, 2896 (1996).
- ²⁰Nanoprobe, Digital Instruments, Santa Barbara, CA.
- ²¹A. Fogden and L. R. White, J. Colloid Interface Sci. **138**, 414 (1990).
- ²²R. W. Carpick, N. Agrait, D. F. Ogletree, and M. Salmeron, Langmuir **12**, 3334 (1996).
- ²³M. Binggeli and C. M. Mate, Appl. Phys. Lett. **65**, 415 (1994).
- ²⁴J. A. Taylor, J. Vac. Sci. Technol. A **9**, 2464 (1991).
- ²⁵M. Tortonesi, Park Scientific Instruments Inc., Sunnyvale, CA (personal communication).
- ²⁶L. E. McNeil and M. Grimsditch, J. Phys. Condens. Matter. **5**, 1681 (1992).
- ²⁷N. Agrait, G. Rubio, and S. Vieira, Phys. Rev. Lett. **74**, 3995 (1995).
- ²⁸P. Tangyunyong, R. C. Thomas, J. E. Houston, T. A. Michalske, R. M. Crooks, and A. J. Howard, Phys. Rev. Lett. **71**, 3319 (1993).
- ²⁹S. S. Sheiko, M. Möller, E. M. C. M. Reuvekamp, and H. W. Zandbergen, Phys. Rev. B **48**, 5675 (1993).